Liquid Crystals
Publication details, including instructions for authors and subscription information:
http://www.informaworld.com/smpp/title~content=t713926090

Two ferroelectric phases of a columnar dibenzopyrene

Harald Bock[a]; Wolfgang Helfrich[a]
[a] Fachbereich Physik, Freie Universität Berlin, Berlin, Germany

To cite this Article Bock, Harald and Helfrich, Wolfgang(1995) 'Two ferroelectric phases of a columnar dibenzopyrene', Liquid Crystals, 18: 3, 387 — 399
To link to this Article: DOI: 10.1080/02678299508036636
URL: http://dx.doi.org/10.1080/02678299508036636

LIQUID CRYSTALS, 1995, VOL. 18, NO. 3, 387–399

Two ferroelectric phases of a columnar dibenzopyrene

by HARALD BOCK* and WOLFGANG HELFRICH
Fachbereich Physik, Freie Universität Berlin, Arnimallee 14,
14195 Berlin, Germany

(*Received 3 June 1994; accepted 1 August 1994*)

The ferroelectric switching of columnar 1,2,5,6,8,9,12,13-octakis-((*S*)-2-heptyloxypropanoyloxy)dibenzo[e,l]pyrene was studied in detail between 60°C and the clearing point 115°C. The switching angle (optical tilt angle) is ± 24·5° up to 10 V μm^{-1} and ± 37° at higher field strengths. The electric polarization is 60 nC cm^{-2} in the low field phase and 180 nC cm^{-2} in the high field phase. The switching rate has apparent activation energies that increase with voltage from 3×10^{-19} to 10^{-18} J. It varies roughly with a power of the voltage, the exponent increasing with decreasing temperature from 2 to 5. At equal voltages, switching is faster in the low field than in the high field phase. We tentatively infer the structures of the two columnar lattices from the ratio of polarizations and other data. From the switching angles, we calculate a tilt angle of 44° for the aromatic cores of the disc-like molecules stacked in the columns. Finally, we point out possible advantages of ferroelectric columnar liquid crystals over their smectic counterparts in electro-optical displays.

1. Introduction

Liquid crystals may be divided into three classes: three-, two- and one-dimensional fluids, which are called nematic, smectic, and columnar mesophases, respectively. In 1970, the electro-optically switchable twisted nematic cell was invented [1] which underlies most of today's liquid crystal displays. In 1974, Meyer *et al.*, discovered the ferroelectricity of tilted chiral smectic phases [2] which is used in the bistable, very fast-switching displays invented in 1980 by Clark and Lagerwall [3].

After columnar phases had been discovered by Chandrasekhar *et al.*, in 1977 [4], it was soon realized that they can be ferroelectric if the disc-like molecules are chiral and tilted with regard to the axis of the column [5]. In such phases, every column has a spontaneous polarization perpendicular to its axis. The columnar phase is ferroelectric whenever the polarizations do not neutralize each other. However, electric realignment of ferroelectric columnar phases was thought to be impossible for many years [6] and even the existence of a bulk polarization was doubted [7].

Recently, we reported in a short communication that ferroelectric switching takes place in the columnar state of a dibenzopyrene with eight alkyl lactic acid chains and explained how tilting these chiral discotic molecules can produce a strong ferroelectric dipole moment [8]. We now present detailed data on the electro-optical behaviour of a homologous compound, 1,2,5,6,8,9,12,13-octakis-((*S*)-2-heptyloxypropanoyloxy)dibenzo[e,l]pyrene to be designated D8m*10 (see figure 1). (We use the following abbreviation scheme for such ester discotics: the capital letter denotes the core, and is followed by the number of chains; the small letter denotes the nature of the chain, and

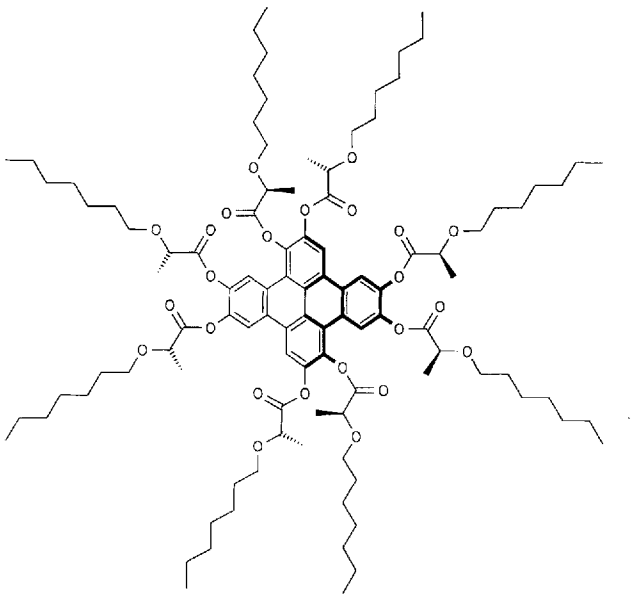

Figure 1. D8m*10 molecule with tilted aromatic core. The orientation of the core within its plane is arbitrary. The tilt axis is vertical, the tilt direction points to the left, and the direction of the molecular dipole moment, which may be identified with the mean direction of carbonyl dipoles, points downwards and is parallel to the tilt axis.

* Author for correspondence.

is followed by the chain length; an asterisk marks chiral cores or chains. D stands of dibenzopyrene, m of lactic acid.) It differs from the previous molecule, D8m*9, only by an additional methylene unit in the hydrocarbon chains.

In the following, we first describe the synthesis of the mesomorphic material. The experimental section begins with the calorimetric properties of the mesogen and the optical appearance of its columnar state. There are two columnar phases, one at low and the other at high electric fields, which differ in their physical properties. The electro-optical switching angles, the switching times, and the ferroelectric polarizations have been measured as functions of voltage and temperature. Noting that the polarization is three times larger in the high field than in the low field phase, we select in the Discussion types of lattices of elliptic and polarized columns that can underlie the two phases. On the basis of a simple model for the optical dielectric tensor, we calculate the tilt angle of the molecular aromatic cores in the columns. Yielding the same value for the two phases, the calculation confirms the selection. Further arguments restrict the choice to a few pairs of lattices, with a preference for a single one. In the Conclusion, we consider the possible advantages and disadvantages of ferroelectric columnar liquid crystals in electro-optical displays as compared to ferroelectric smectics.

2. Synthesis

2, 5, 6, 9, 12, 13-Hexamethoxydibenzo[e,l]pyrene-1, 8-quinone was synthesized in three steps by the procedure of Musgrave and Webster [9, 10] (first, iodination of veratrole with I_2 and HgO, second, an Ullmann reaction to give 3,3′,4,4′-tetramethoxybiphenyl, and third, oxidative dimerization with *p*-chloranil in sulphuric acid).

1 g of this hexamethoxyquinone was stirred in 50 ml of dry benzene, 3 ml of boron tribromide were added, and the mixture was heated under reflux for 2 hours. The mixture was poured into 300 ml of ice cold water and stirred for 1 hour. The product—hexahydroxydibenzopyrenequinone (0·8 g)—was filtered off and dried under vacuum at 50°C.

To 0·5 g of the above product in 40 ml of dry tetrahydrofuran and 10 ml of dry pyridine, 2 g of zinc dust and 5 g of (S)-*O*-heptyl-lactic acid chloride were added with ice bath cooling. The mixture was stirred for 3 hours at room temperature, then diluted with 200 ml of dichloromethane. The zinc was filtered off, and the solution washed first with dilute hydrochloric acid and then with water. The organic phase was dried with sodium sulphate, the solvent evaporated and the mixture containing the product was twice chromatographed in dichloromethane solution on silica gel; the product was precipitated with ethanol, chromatographed again, precipitated again and dried under vacuum at 50°C. Yield: 0·3 g of D8m*10.

(S)-*O*-heptyl-lactic acid chloride was obtained in more than 90 per cent yield from ethyl (S)-*O*-heptyl-lactate by stirring for a day in an excess of methanolic potassium hydroxide solution, evaporating the solvent, acidifying with an excess of dilute hydrochloric acid, extracting into ethyl acetate, drying the solution with sodium sulphate, evaporating the ethyl acetate, stirring for three hours in a tenfold excess of thionyl chloride with three drops of dimethylformamide, and evaporating the thionyl chloride at 50°C and 20 mbar. The acid chloride was immediately used to prevent racemization.

The alkylated ethyl acetate was obtained in *c.* 60 per cent yield by stirring silver(I) oxide with an excess of 1-iodoheptane and an excess of ethyl lactate in dry tetrahydrofuran for 36 h at 50°C in the dark, filtering off the silver salts, evaporation the solvent and chromatography in dichloromethane solution on silica gel.

3. Experiments

D8m*10 as synthesized changes from a columnar phase to the isotropic liquid at about 115°C, with an enthalpy of $11{\cdot}8\,J\,g^{-1} = 21{\cdot}1\,kJ\,mol^{-1}$ (heating, $10\,K\,min^{-1}$). The phase transition was spread (in half peak widths) over *c.* 5 K above and 2·5 K below a common starting point when the temperature was raised and lowered, respectively, at $10\,K\,min^{-1}$. We think the considerable spreading is attributable to the size of the molecules and the complexity of the columnar order, rather than impurities. No other phase transition above − 25°C could be detected by differential scanning calorimetry (DSC) (The sensitivity of our DSC apparatus was $2\,Jmol^{-1}K^{-1}$. We reported in our earlier work [8] a melting point for D8m*9, because we observed a very weak peak in the first DSC heating run. When the experiments were repeated some days later, the weak peak reappeared, with its intensity depending on the time between the two measurements. We believe this to be a sign of very slow and incomplete crystallization. Because we did not observe such a crystallization peak with D8m*10, we preferred to use the longer homologue for detailed measurements. Based on our present experience with highly viscous columnar liquid crystals, we place the clearing and melting temperatures of D8m*9 at 118°C and roughly 80°C, respectively; the enthalpy of clearing is $12\,J\,g^{-1} = 20\,kJ\,mol^{-1}$ (DSC, heating, $10\,K\,min^{-1}$, similar smearing as D8m*10).) In particular, no glass transition was found, although the substance is completely rigid at low temperatures. Shear is not possible at room temperature, while at temperatures around 100°C the sample is easily sheared between glass plates. Shearing is the only method which we found to obtain a uniform alignment of the columns. The texture (between crossed polarizers) of

the mesophase that appears spontaneously when the isotropic liquid is cooled consists of characteristic flower-like domains [4] and some grey to black areas. In the flowers, the columns are parallel to the glass and form circles around the flower centres [11]. The black extinction crosses giving the impression of flowers are seen because the liquid crystal does not change the polarization of transmitted light where the principal axes of its dielectric tensor in the plane of the cell coincide with the polarizer and analyser directions. If the disc-like molecules are tilted with respect to the column axis, and if the tilt direction has a component parallel to the glass, the black brushes of the extinction cross make an angle with the polarizer and analyser directions, the optical tilt angle. Freshly prepared samples (see figures 2 and 3), do not show any optical tilt angle, apparently because the two-dimensional lattice of columns is still disordered, at least as far as concerns the two opposite polarities that each elliptic column can assume in the lattice. However, an optical tilt angle develops in the course of time, indicating true ferroelectricity. In the grey to black areas, the columns probably stand up on the glass.

When the sample is switched back and forth for some minutes, the grey to black areas disappear in favour of expanding flowers, and the full optical tilt angle is uniformly established. This texture has a good birefringence and is stable at zero field. The total polarization should now be oriented more or less normal to the conducting cell walls. Shearing leads to a rather uniform alignment of the columns parallel to the glass and parallel to the direction of shear [12]. The full optical tilt angle of sheared samples is the same as in the flowers. When an alternating voltage is applied, the optical tilt angle reverses with the field, going through an optically untilted state. We checked with a phase retardation plate that the direction of maximum refractive index for transmitted light is normal to the columns in this state. As the molecular tilt direction is perpendicular to the tilt-induced molecular dipole, the optical tilt vanishes when the total ferroelectric polarization in the field direction reaches zero. The optical tilt angle rotates counter-clockwise when the voltage on the side of viewing changes from negative to positive, as was also found earlier with the homologous compound D8m*9 [8]. This sense of the rotation agrees with the tilted molecular structure depicted in figure 1.

The samples display a field-induced phase transition at about $10\,V\,\mu m^{-1}$ (see figures 4–6). The high field phase relaxes rather slowly to the low field phase when the field is turned off. Therefore, switching times and ferroelectric polarizations could be measured for both phases for field strengths near $10\,V\,\mu m^{-1}$. The high field phase is easily distinguished optically from the low field phase by a higher refractive index anisotropy and by a larger optical tilt angle. The anisotropy of the refractive index for

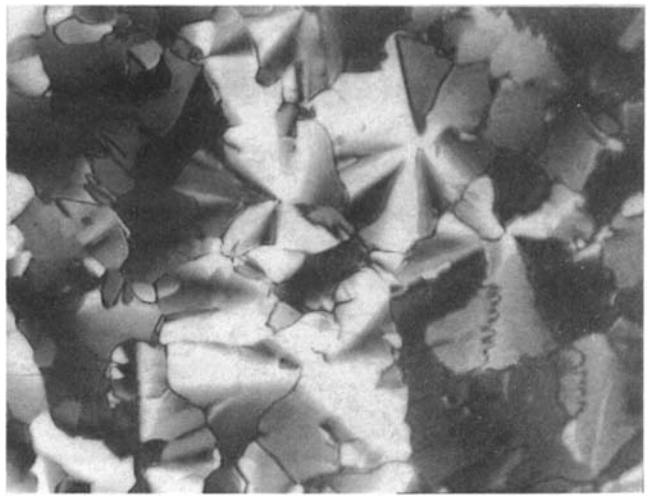

Figure 2. Virgin texture after slow cooling ($0{\cdot}5\,K\,min^{-1}$ from the isotropic liquid ($10\,\mu m$). Field of view *c.* $800 \times 600\,\mu m$.

Figure 3. Virgin texture after fast cooling ($20\,K\,min^{-1}$) from the isotropic liquid ($10\,\mu m$). Field of view *c.* $400 \times 300\,\mu m$.

transmitted light, $(\Delta n)_{trans}$, was estimated for the low field and high field phases from the colours between crossed polarizers—first order yellow and second order green in $10\,\mu m$ cells—to be $(\Delta n)_{trans} = 0{\cdot}03$ and $(\Delta n)_{trans} = 0{\cdot}075$, respectively. A 'triangular' voltage and the ensuing intensity of transmitted light are plotted together versus time for the low and the high field phases in figure 7.

Precise values of the optical tilt angles in both phases were obtained directly from the flower texture between crossed polarizers by measuring on a video monitor the rotation of the typical black extinction brushes [11] in a rectangular alternating field (see figures 4 (*a*), (*b*) and 6 (*a*), (*b*)). This simple method yielded good results when

(*a*)

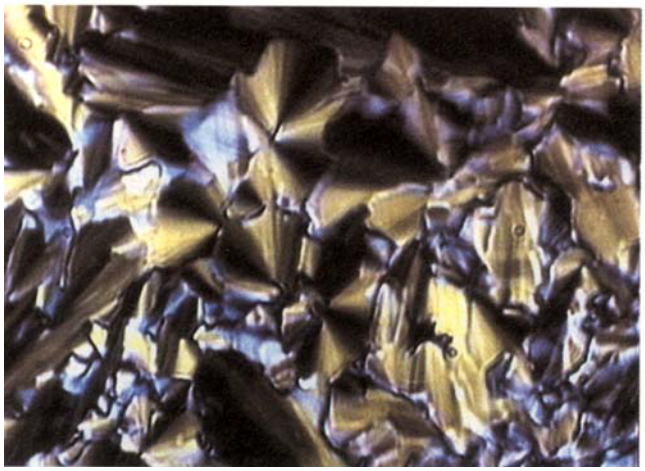

(*b*)

Figure 4. (*a*), (*b*), The two fully switched states in the low field phase (10 μm). Field of view *c*. 200 × 150 μm.

(*a*)

(*b*)

Figure 6. (*a*), (*b*) The two fully switched states in the high field phase (10 μm). Field of view *c*. 200 × 150 μm.

Figure 5. During the relaxation from the high field to the low field phase after the voltage was turned off (10 μm). Field of view *c*. 200 × 150 μm.

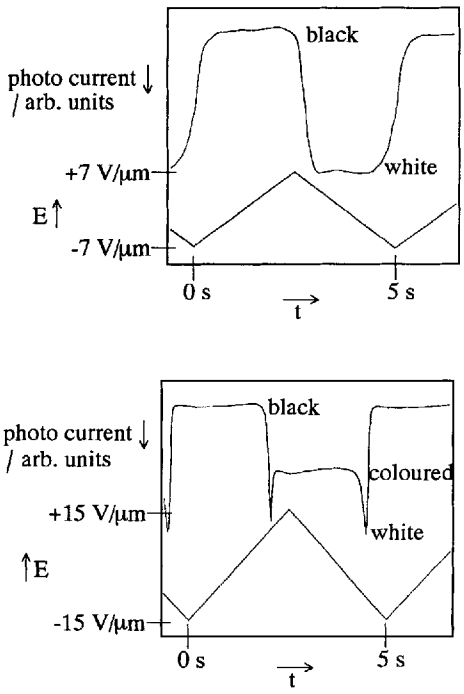

Figure 7. Triangular voltage and light intensity versus time. Sheared cell (roughly 10 μm thick), crossed polarizers, 22·5° between polarizer and shear direction, 100°C, 0·2 Hz. Top: low field phase (peak field: *c.* $\pm$ 7 V μm^{-1}). Bottom: high field phase (peak field: *c.* 15 V μm^{-1}).

the measurement was carried out for the same flower-like domain for three different polarizer cross orientations (progressing in steps of 30°). While the measurements at the three positions differed considerably, apparently because of asymmetries in the domain growth, their mean value varied only within 1° from domain to domain. The optical tilt angles of both phases show no significant temperature dependence and were (24·5 $\pm$ 1)° and (37 $\pm$ 1)° (see figure 8).

If in the low field phase the field is turned off during the switching process, the optical tilt angle can be arrested anywhere between + 24·5° and − 24·5°, providing the switching is slow enough. These intermediate states seem stable for hours or days.

We studied the dependence of the switching time on electric field strength E and temperature T by measuring the time between rectangular voltage reversal and polarization current maximum [13] (see figure 9). Some of our samples were electrically stable even at 50 V μm^{-1}, permitting us to carry out systematic measurements up to that field strength. Below 20 V μm^{-1}, electric breakthroughs generally did not occur.

The field dependence of the switching time τ is extreme, $1/\tau$ being approximately proportional to E^4 over a wide range of voltages and temperatures (see figure 10). Whenever switching time for both phases could be

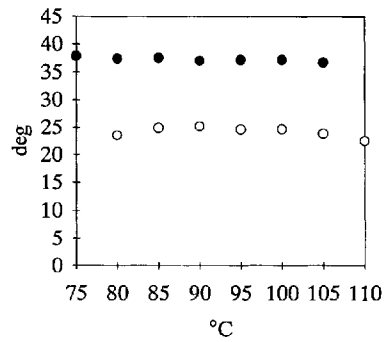

Figure 8. Full optical tilt angle versus temperature. Solid dots: high field phase. Open dots: low field phase.

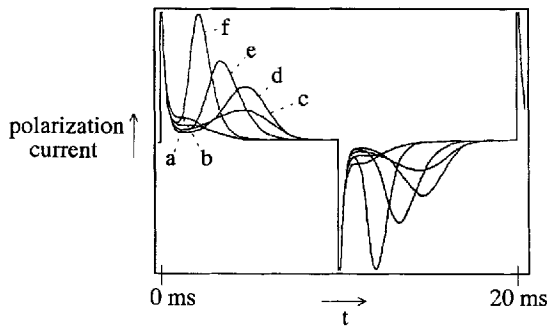

Figure 9. Polarization current versus time at different rectangular voltages. Voltages increases from (*a*) to (*f*), with the field strengths varying in a rather narrow range around 10 V μm^{-1}, 104·2°C, 50 Hz, 10 μm. Notice that the phase transition from the faster low field phase to the slower high field phase increases the polarization.

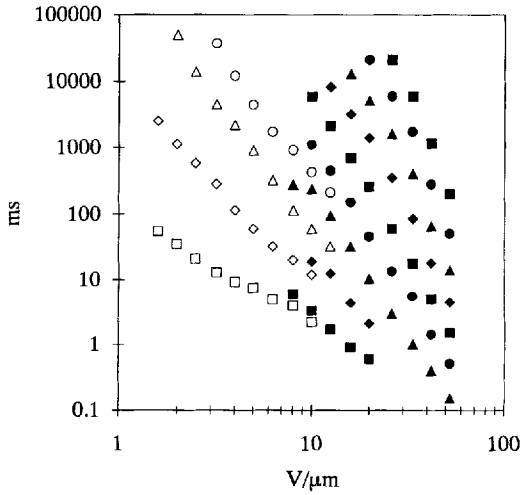

Figure 10. Field dependence of the switching time at the inverse temperatures (from bottom to top) 2·6, 2·65, 2·7, 2·75, 2·8, 2·85, 2·9, 2·95, and $3{\cdot}0 \times 10^{-3}\,K^{-1}$. Solid symbols: high field phase. Open symbols: low field phase.

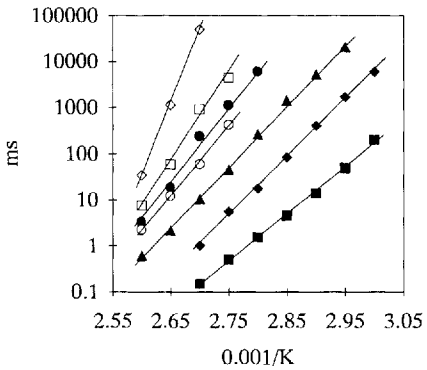

Figure 11. Temperature dependence of the switching time at the field strengths (from top to bottom) 2, 5, 10, 20, 33, and 53 V μm^{-1}. Solid symbols: high field phase. Open symbols: low field phase. Note that both phases occur for 10 V μm^{-1}.

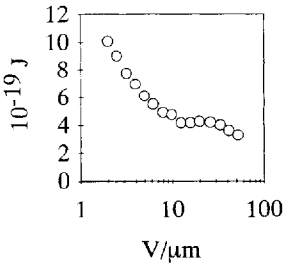

Figure 12. Field dependence of the apparent activation energy of switching.

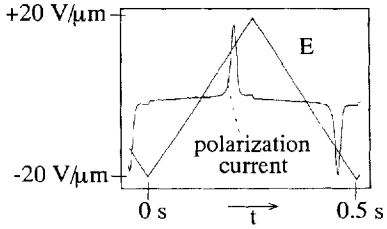

Figure 13. Triangular voltage and resulting polarization current versus time. 104·2°C, 10 μm, 2 Hz, peak field: $\pm$20 V μm^{-1}, high field phase.

measured at the same field strength, the low field phase was up to five times faster than the high field phase (see figure 9). Finding ln τ to increase roughly linearly with $1/T$ (see figure 11), we computed apparent activation energies between 3×10^{-19} J and 10^{-18} J for different field strengths (see figure 12). Ferroelectric polarizations at different temperatures were measured by integrating the polarization current peak in a triangular alternating field [14] (see figure 13). At high frequencies, the values thus obtained fitted well with the hysteresis heights of the Sawyer–Tower method [15] (see figure 14), but the latter proved unsuitable at low fields which required frequencies below 20 Hz. The polarizations of the low and high field phases are $c.60$ and $c.180$ nC cm^{-2}, respectively, being only slightly temperature dependent, except near the clearing point (see figure 15). Interestingly, the ratio of the two polarizations appears to be an integer, namely three. The independence of temperature holds particularly well for the ratios between the two phases of the polarizations and the optical tilt angles, as is illustrated by figure 16.

The relaxation time from the high to the low field phase, defined as the time required by the optical tilt angle for a 90 per cent return to its low field value, was obtained from the rotation of the black extinction cross in the flower-like

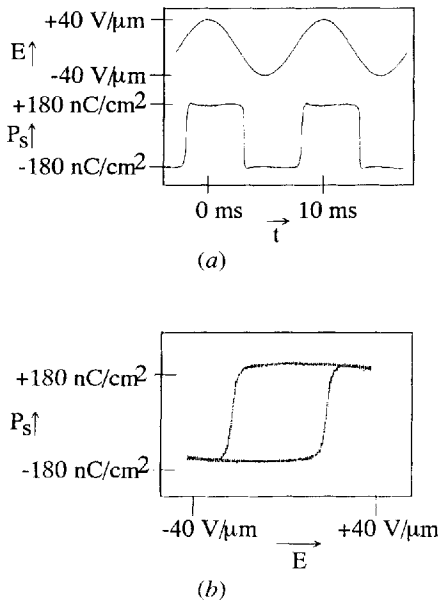

Figure 14. Sawyer-Tower method [15] signal with sinusoidal voltage. 97·2°C, 100 Hz, 2 μm, peak field; $\pm$ 40 V μm^{-1}, high field phase. Top: applied voltage and polarization versus time. Bottom: polarization versus applied voltage.

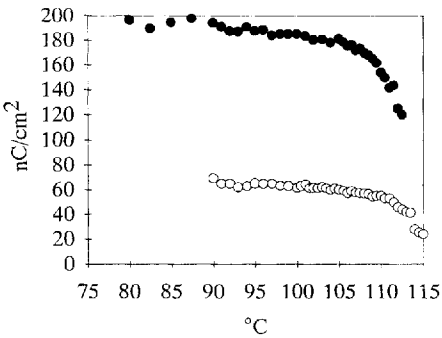

Figure 15. Temperature dependence of the polarization. Solid dots: high field phase. Open dots: low field phase.

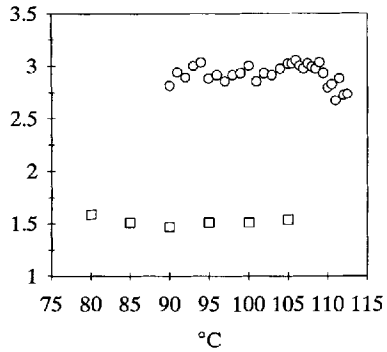

Figure 16. Ratios versus temperature. Circles: ratio between high and low field phase polarizations. Squares: ratio between high and low field phase tilt angles.

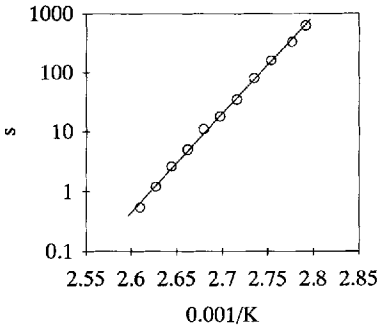

Figure 17. Temperature dependence of the 0 to 90 per cent relaxation time from the high field to the low field phase.

domains after the field was turned off. The measurements were carried out with a CCD camera mounted on the microscope, a video monitor, and a stop-watch. A cross on a transparency was attached to the monitor so that its centre coincided with that of a flower domain, and was set at 26° (the optical tilt angle of the low field phase plus 10 per cent of the difference between the two optical tilt angles). The logarithm of the relaxation time from the high to the low field phase increases linearly with $1/T$, indicating an apparent activation energy of $5{\cdot}2 \times 10^{-19}$ J $\pm$ 5 per cent (see figure 17).

4. Discussion

4.1. *Reversing the molecular tilt*

When the normals to the aromatic cores of the discotic molecules make an angle with the axis of the column, the molecules and, thus, the column as a whole may acquire electric dipole moments. This is because the tilt, resulting from repulsion between chains and attraction between cores [16], is essentially restricted to the aromatic cores of the disc-like molecules [6]. Therefore, part of the chains of each molecule make an angle with the plane of the tilted core. If the centre of chirality is where the chain deflects, nearby bonds with an electric dipole moment (for example, carbonyl groups or ether bonds) can give rise to a non-zero time averaged molecular and columnar dipole moment. If in addition, the chains are equal and identically attached, these dipole moments will have the same sign for all the deflected chains. For reasons of symmetry, the total molecular dipole moment must on average be perpendicular to both the axis of the column and the tilt direction, thus being parallel to the axis about which the disc rotates when it tilts.

Two of the possible mechanisms of reversing the columnar polarization are similar to those in ferroelectric smectics. In one case, the column (or part of it) rotates as a whole around the axis of the column. In the other case, the tilt reverses through an untilted state, but there is no molecular rotation around the column axis. A third mechanism, proposed to us by Xinhua Chen, is different: the molecular tilt direction, but not the molecules themselves rotates around the column axis. This may be compared with a coin rotating on its rim on the table without (much) changing the orientation of the head depicted on its upper side. In the first mechanism, there is considerable friction between the rotating columns, but none within them. The second mechanism involves an intermediate conformation in which the elliptic cross-section of the column widens to a circle. It is probably associated with a considerable stress in the column and the surrounding lattice, which implies a high energy barrier. There is friction between adjacent molecules in the columns and between columns as part of the hydrocarbon chains move up and down along the column. The same two kinds of friction occur in the third mechanism, but all chains move, and shear between molecules is in two directions. We do not know which of the three mechanisms dominates in ferroelectric switching. Among other things, the friction coefficient acting between cores will be important.

Examination under the microscope suggests that probably does not require the motion of domain boundaries. While domains are seen to emerge, grow and coalesce during switching, the gradual rotation of the optical tilt angle seems to take place regardless of the local presence or absence of domain walls.

4.2. *Switching in a quasi-hexagonal lattice*

The two-dimensional Bravais lattices of most columnar phases known to date are nearly hexagonal. The deviation from hexagonality, defined as the deviation from $\sqrt{3}$ of the ratio between the lengths of the two sides of a rectangular two column unit cell, is below 10 per cent in most cases. (Greater deviations from hexagonality were observed only with mesogens such as benzoyloxy-triphenylenes whose peripheral groups bear aromatic units) [17].

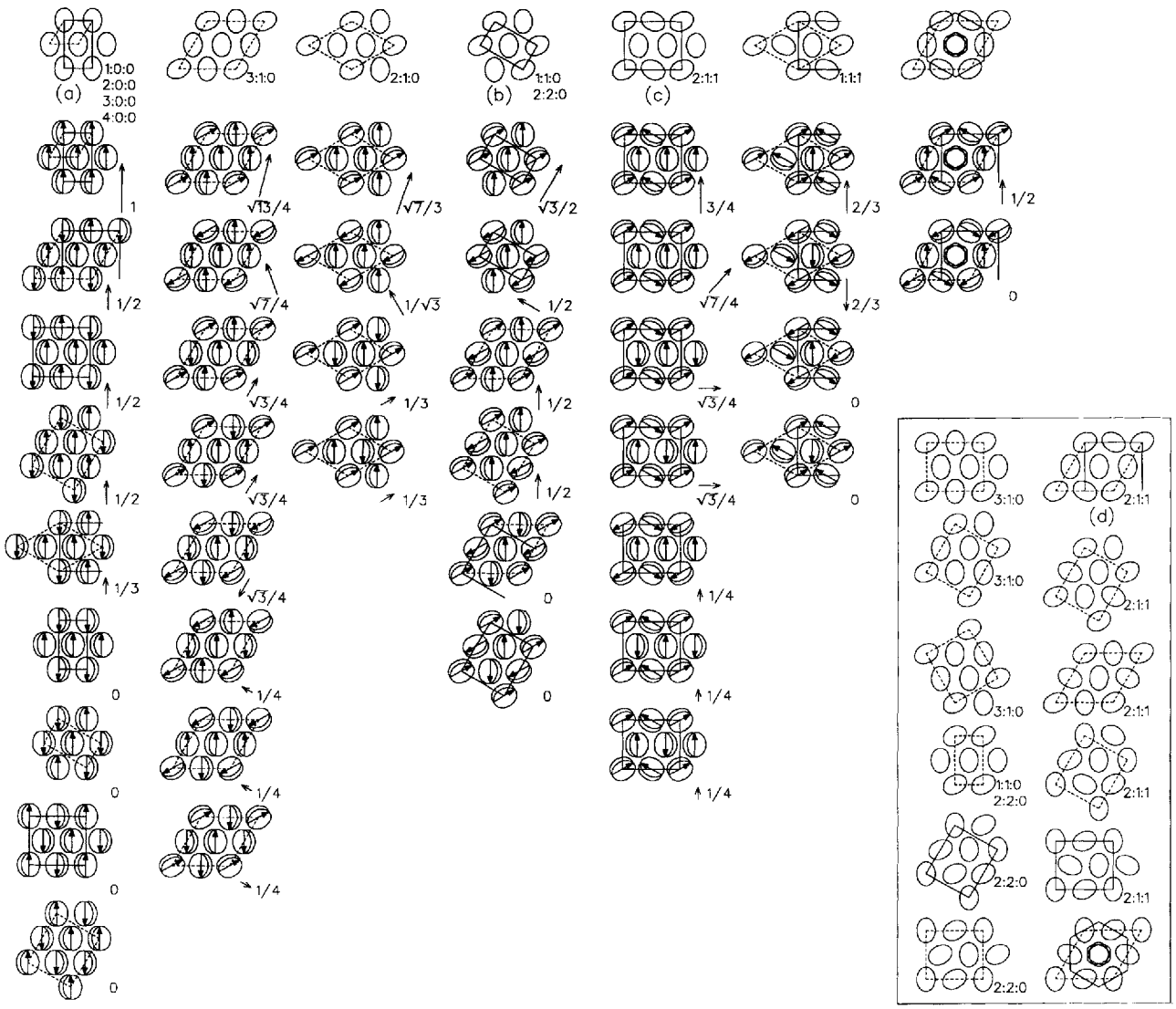

Figure 18. Quasi hexagonal ellipse lattices and their variations for tilted polar columns. View along column axes. Ratios of differently oriented ellipses and relative polarizations are indicated. Rectangular unit cells are drawn with full lines, oblique unit cells are drawn with dashed lines. Where the rectangular unit cell is too big to be shown, both the smaller oblique unit cell and half of the rectangular unit cell are drawn.

In a hexagonal lattice, each column has six nearest neighbours like itself. Tilt destroys this simple hexagonality, as it gives the columns an elliptic cross-section and, if the molecules are chiral, a ferroelectric polarization. The major axis of the ellipse is assumed to be normal to the direction of tilt, thus coinciding with the direction of polarization. For steric reasons, we may expect six preferred tilt directions, namely those in which the polarization (major axis) points to a gap between the six nearest columns or, in other words, to one of the next nearest columns.

Figure 18 displays simple quasi-hexagonal lattices that can be built from ellipses aligned toward a next nearest neighbour. Starting from non-polar ellipses with three distinguishable alignments, one obtains the complete picture with six preferred directions of each ellipse by introducing polarity along the major axes. We have tried to compile all lattices containing two, three and four columns in the primitive unit cell, apart from the following exceptions. We omit rows of four columns and other unit cells whose lengths are more than twice their width. Lattices that can be transformed into each other by rotating the liquid crystal in three-dimensional space are shown only in one view. While the non-polar lattices of ellipses are supposed to be complete, the associated polar lattices are shown only for one representative of each class, as

characterized by the numbers of different ellipses in a unit cell (for example 2:1:1). Figure 18 also shows two cases of truly hexagonal ordering, with one column in the unit cell of four being of circular cross section. (The simple hexagonal lattice is omitted as its unit cell consists of a single circle.) The lattices of non-polar ellipses that so far have been invoked to interpret X-ray data are marked with the letters (*a*) to (*c*) in figure 18. The most common of them (apart from truly hexagonal) is the herringbone pattern (*b*), with 1:1:0 [17]. Uniformily directed tilt (*a*) seems rare [17] and the only example of 2:1:1 has been assigned to the pattern (*c*) [18]. Moreover, a complex hexagonal lattice similar to those shown in figure 18 has also been discovered [6]. It does not appear in figure 18 because the ellipses, polar in that case, were assumed to point to a nearest neighbour, while they would have to point to a next nearest neighbour in our restricted scheme. Except for the complex hexagonal lattices, the hexagonal symmetry is broken in the non-polar and polar lattices of figure 18. Centred rectangular lattices are indicated by both primitive and rectangular unit cells. Many of the lattices are oblique for reasons of symmetry. It should be noted that lattice distortion may also arise from reasons other than symmetry, as in an oblique version of (*b*) [17].

The ferroelectric polarization of every quasi-hexagonal lattice of polar ellipses in indicated in relative units by an arrow and an absolute value. In a sample cell, the lattice of columns probably prefers an orientation where rows (layers) of nearest neighbour columns are parallel to the glasses serving as electrodes. The effective polarization of ferroelectric switching would be slightly smaller than the full value in cases where the polarization is not quite perpendicular to the most suitable set of such rows.

Inspection of figure 18 reveals a number of possibilities (with one exception, all of type 2:1:1) to exactly triple the ferroelectric polarization of the liquid crystal without changing the lattice of non-polar ellipses. The lattices can be oriented in such a way, with rows of columns along the boundaries, that the polarization is normal to the glasses. Four possibilities of type 2:1:1 are shown in figure 19, the non-polar lattices being equal for *A* and *B* and for *C* and *D*, respectively. In cases *A* and *B*, the rows of predominant ellipses are parallel to the glass, whereas in cases *C* and *D*, they are not. A different view of the columns is given for *A* and *B* in figure 20. The tripling comes about by an antiferroelectric–ferroelectric transition of the predominant ellipses in cases *A* and *C*, whereas it results from a joint reversal of polarity of the two kinds of less frequent ellipses in cases *B* and *D*. From the switching behaviour, we cannot distinguish between the two ellipse lattices, but we can distinguish between the antiferroelectric–ferroelectric transition (*A*, *C*) and the joint reversal of polarity (*B*, *D*) in the following way. The observation that the transition to the high field phase is linked with an increase of the switching time is not plausible in cases *B* and *D*. It can be explained for cases *A* and *C* where switching in the low field phase does not require the reversal of the columnar dipoles (see figure 20). Instead, the switching can be achieved at fixed polarities of the vertical ellipses by 60° rotations of the oblique ellipses. The columns with vertical ellipses have to participate in the switching only in the high field phase, and slow down the process because the field initially has no lever to turn them.Two other possibilities of tripling the polarization are provided by the phase transitions *E* and *F* of figure 19, which both start from lattices containing three columns per unit cell. They may again be ruled out, as they fail to explain the faster switching in the low-field phase. Moreover, the lattice parameters are likely to change considerably in transition *F* which realigns two of the ellipses. This should result in a disruption of columnar order, which was not observed. A tripling of the polarization can, in principle also be obtained with all 2:2:0 lattices if they are aligned with the right rows of nearest neighbour columns parallel to the boundaries. However, the ferroelectric polarization then inevitably has a component parallel to the electrodes so that an electric field may be expected to realign the lattice of columns in the course of time. Since no signs of such an effect have been noticed during our experiments, we dismiss 2:2:0 lattices.

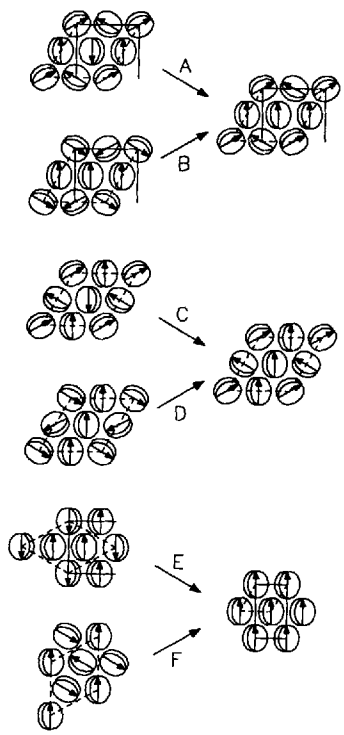

Figure 19. Phase transitions tripling the polarization. View along column axes.

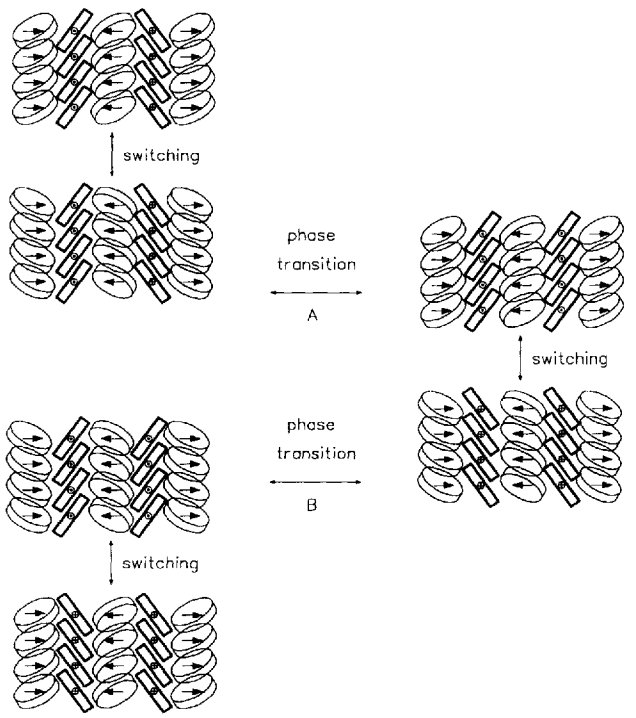

Figure 20. Cases A and B seen in direction of light. The second and the fourth of the five columns lie on top of the other three.

Cases *A* and *B* in figure 19 and 20 belong to the non-polar lattice (*d*) in figure 18. We prefer (*d*) over the similar (*c*), although it is (*c*) that has been found previously [18]. In the present case of strongly polarized columns, the arrangement of their dipole moments should play an important role. The dipolar interaction energy at zero electric field seems to be at its absolute minimum in the low field phase of case *A* which belongs to (*d*). It is clearly larger in the corresponding dipolar lattice of (*c*) displayed at the bottom of the vertical row in figure 18. The differences in dipolar energy appear less significant for the high-field phases. For a reliable prediction of the structure, one needs to know the total interaction energy between columns. In our previous paper [8], we suspected that the field-induced phase transition converts a herring-bone pattern into a uniformily tilted lattice with one column per unit cell, which would be of type (*a*) in figure 18 with 1:0:0. After measuring the ratio of the polarizations, we cannot maintain this interpretation.

4.3. *From the switching angle to the molecular tilt angle*

It is interesting to calculate, on the basis of a simple model, the molecular tilt angle in the columns from the optical tilt angle which is the switching angle. This permits, in addition, a check of structural assignments, since the same molecular tilt angle should be obtained for the low- and high-field phases. We will study in detail case *A* of figure 19 and then draw some general conclusions.

For the calculations, we introduce the right-handed cartesian coordinate system sketched in figure 21. The z axis is parallel to the columns and thus to the glass; the x axis is also parallel to the glass, while the y axis is normal to it. the tilt angle ϑ, a polar angle, may be defined as the angle which the director of the normals to the molecular cores makes with the z axis. The azimuth φ of this director in the x, y plane, as measured from the x axis is, at the same time, the angle of the spontaneous molecular dipole moment as measured from the y axis. Finally, the angle χ, measured from the z axis in the z, x plane, designates the direction of polarization of incoming light which is thought to propagate along the y axis. With ε_{zz}, ε_{xx} and $\varepsilon_{zx} = \varepsilon_{xz}$ being elements of the optical dielectric tensor of the liquid crystal, the dielectric constant felt by light passing through the sample between parallel polarizers of angle χ is given by

$$\varepsilon(\chi) = (\cos\chi, \sin\chi)\begin{pmatrix}\varepsilon_{zz} & \varepsilon_{zx}\\ \varepsilon_{xz} & \varepsilon_{xx}\end{pmatrix}\begin{pmatrix}\cos\chi\\ \sin\chi\end{pmatrix}$$
$$= \varepsilon_{zz}\cos^2\chi + 2\varepsilon_{zx}\cos\chi\sin\chi + \varepsilon_{xx}\sin^2\chi.$$

It has it maxima and minima at the four orthogonal angles where $d\varepsilon(\chi)/d\chi = 0$, i.e.

$$\frac{\cos^2\chi - \sin^2\chi}{\cos\chi\sin\chi} = \frac{\varepsilon_{zz} - \varepsilon_{xx}}{\varepsilon_{zx}}. \qquad (1)$$

The solutions of this equation are the polarization

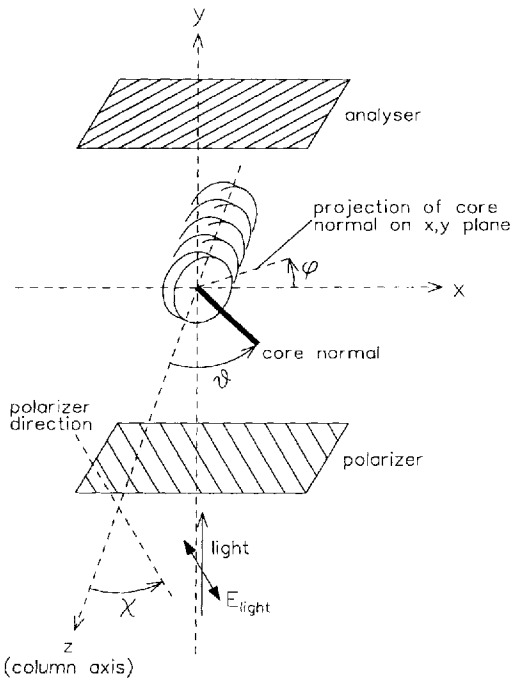

Figure 21. Definition of coordinate axes and angles.

directions of maximum extinction when the polarizers are as usual crossed.

In order to calculate the elements of the dielectric tensor, we first need an expression for the tensor of a single column or, more precisely, of a liquid crystal consisting of columns with one and the same tilt direction. The dielectric properties of homogenous systems will be needed to calculate approximately those of the actual liquid crystal with different tilt directions of the columns. Let us assume that the dielectric tensor of a liquid crystal consisting of equally tilted columns can be divided into two parts: an isotropic part ε_{is} and a uniaxial part ε_{ax} along the director of the core normals. This simple form presupposes random orientation of the elongated molecular cores in their plane normal to the director. Because of the aromatic character of the cores, ε_{ax} may be expected to be negative, in agreement with the sign of the measured refractive index anisotropy, $(\Delta n)_{trans}$.

In order to obtain simple formulae for the dielectric tensor elements, we will imagine the liquid crystal to consist of flat sheets parallel to the z,x plane, each representing one of the horizontal rows of columns of figure 19. There may be one type or two alternate types of sheets. For convenience, we will take from now on each column to be dielectrically homogenous and of rectangular cross section. Oblique and vertical ellipses are distinguished by the indices ob and vt, respectively.

The model of sheets is particularly easy to apply to case *A* of figure 19 where the sheets contain either oblique or vertical ellipses only and the oblique ellipses alternate in tilt direction. This permits us to treat applied fields in the z and x direction as uniform although local fields, by definition fields of zero average, still exist in directions perpendicular to the applied field. According, we may express the dielectric tensor elements of the liquid crystal by the mean values of the contributions of the two kinds of sheets,

$$\varepsilon_{zz} = (\varepsilon_{zz,ob} + \varepsilon_{zz,vt})/2,$$

$$\varepsilon_{xx} = (\varepsilon_{xx,ob} + \varepsilon_{xx,vt})/2,$$

and

$$\varepsilon_{zx} = (\varepsilon_{zx,ob} + \varepsilon_{zx,vt})/2.$$

For the *low field phase of A* we expect

$$\varepsilon_{zz,ob} = \varepsilon_{is} + \varepsilon_{ax}\cos^2\vartheta,$$

$$\varepsilon_{zz,vt} = \varepsilon_{is} + \varepsilon_{ax}\cos^2\vartheta - \frac{(\varepsilon_{ax}\cos\vartheta\sin\vartheta)^2}{\varepsilon_{is} + \varepsilon_{ax}\sin^2\vartheta},$$

$$\varepsilon_{xx,ob} = \varepsilon_{is} + \varepsilon_{ax}\sin^2\vartheta\cos^2\varphi,$$

$$\varepsilon_{xx,vt} = \varepsilon_{is} + \varepsilon_{ax}\sin^2\vartheta.$$

$$\varepsilon_{zx,ob} = \varepsilon_{ax}\cos\vartheta\sin\vartheta\cos\varphi,$$

and

$$\varepsilon_{zx,vt} = 0.$$

The last expression, $\varepsilon_{zx,vt}$, vanishes because upward and downward dipole alternate in the sheets of vertical ellipses of the low field phase. The third term of $\varepsilon_{zz,vt}$ represents a correction due to local fields E_x induced by the applied field E_z. (All other corrections due to local fields should be much less.) Inserting $\varphi = \pm 60°$ leads to the mean values

$$\varepsilon_{zz} = \varepsilon_{is} + \varepsilon_{ax}\cos^2\vartheta - (\tfrac{1}{2})\frac{(\varepsilon_{ax}\cos\vartheta\sin\vartheta)^2}{\varepsilon_{is} + \varepsilon_{ax}\sin^2\vartheta},$$

$$\varepsilon_{xx} = \varepsilon_{is} + (\tfrac{5}{8})\varepsilon_{ax}\sin^2\vartheta$$

and

$$\varepsilon_{zx,ob} = (\tfrac{1}{4})\varepsilon_{ax}\cos\vartheta\sin\vartheta.$$

In order to assess the importance of the correlation term of ε_{zz}, we assume the ordinary and extraordinary refractive indices in the case of uniformly tilted ellipses to be $n_o = 1{\cdot}5$ and $n_e = 1{\cdot}4$. The birefringence $\Delta n = n_e - n_o = -0{\cdot}1$ is inferred from the birefringence of the high temperature phase for transmitted light, $(\Delta n)_{trans} = 0{\cdot}075$, which we multiply by 4/3 to simulate uniform tilt. The indices of refraction correspond to $\varepsilon_{is} = n_o^2 = 2{\cdot}25$ and $\varepsilon_{ax} = 2(\Delta n/n_o)\ \varepsilon_{is} = -0{\cdot}3$. Inspection shows that for $\vartheta < 45°$ the correction amounts to no more than 3 per cent of $\varepsilon_{ax}\cos^2\vartheta$.

Neglecting the correction, we arrive at

$$\frac{\varepsilon_{zz} - \varepsilon_{xx}}{\varepsilon_{zx}} = \frac{\cos^2\vartheta - (\tfrac{5}{8})\sin^2\vartheta}{(\tfrac{1}{4})\cos\vartheta\sin\vartheta}. \qquad (2)$$

Similar reasoning for the *high field phase of A* results in the same formulae with two exceptions. There is no correction of ε_{zz} and the formerly vanishing dielectric tensor element becomes $\varepsilon_{zx,vt} = \varepsilon_{ax}\cos\vartheta\sin\vartheta$. This results in $\varepsilon_{zx} = (\tfrac{3}{4})\varepsilon_{ax}\cos\vartheta\sin\vartheta$ and

$$\frac{\varepsilon_{zz} - \varepsilon_{xx}}{\varepsilon_{zx}} = \frac{\cos^2\vartheta - (\tfrac{5}{8})\sin^2\vartheta}{(\tfrac{3}{4})\cos\vartheta\sin\vartheta}, \qquad (3)$$

where the last formula is exact in our approximate model.

Note that the theoretical ratios $(\varepsilon_{zz} - \varepsilon_{xx})/\varepsilon_{zx}$ as given by equations (2) and (3) do not depend on ε_{is}. They differ only in ε_{zx} which is 3 time larger for the high field than for the low-field phase. Substituting for these ratios the expressions obtained from equation (1) and switching angles 24·5° (low field) and 37° (high field), one arrives at the molecular tilt angles $\vartheta = 43{\cdot}96°$ and $\vartheta = 44{\cdot}03°$, respectively.

The reasonable magnitude and, especially, the very good agreement of the two independently determined molecular tilt angles certainly agrees with case *A* of figure 19. Unfortunately, it supports almost equally well the other cases shown in figure 19 and the other 2:1:1 lattices of figure 18. For all of them, ε_{zx} and $\varepsilon_{zx}/(\varepsilon_{zz} - \varepsilon_{xx})$ should be within a few per cent three times larger in the high field than in the low-field phase. It is easy to see that

this tripling is closely related to that of the ferroelectric polarization. The poor dielectric discrimination is due to the smallness of the relative dielectric anisotropy, $|\varepsilon_{ax}|/\varepsilon_{is}$, which is about 0·1. This anisotropy controls all local electric fields, including those in the direction of the applied field. (An apparent field E_x is associated with parallel local fields in case *C* of figure 19, where oblique and vertical columns alternate in each horizontal sheet.) Very precise measurements of the two switching angles and extremely careful modelling would be needed to overcome those difficulties.

4.4 *The switching time*

The switching time ranged from 0·1 ms to 100 s in our experiments, depending strongly on temperature and field strength. The activation energies taken from the Arrhenius plot of figure 11 are between 3×10^{-19} and 10^{-18} J, implying Boltzmann factors from 10^{-26} to 10^{-86} (at 370 K), those energies are too high to represent actual energy barriers except, perhaps, near their lower limit measured at the highest field strengths. (We estimate the collision factor to be less than $10^{12}\,s^{-1}$ and the number of molecules participating as nucleation centres in an activation process to be less than 10^{10}).

The rapid increase of the switching time with decreasing temperature may be taken to suggest a glass transition at a temperature not much below 60°C, the lowest temperature where switching times could be measured. A glass transition has, in fact, recently been found in the columnar phase of similar material by Leisen *et al.* [19]. However, the data of figure 11 do not reveal any systematic deviation from Boltzmann behaviour over the whole range of voltages, and no sign of a glass transition was detected calorimetrically down to − 25°C. The problem of measuring unreasonably high activation energies may be resolved by allowing for a temperature dependence of the true activation energy. Using a linear expansion, we may rewrite the Boltzmann factor as

$$\exp -\left[\frac{E(T_0) + (dE(T_0)/dT)(T - T_0)}{kT}\right]$$

$$= \exp\frac{-dE(T_0)/dT}{k} \exp -\left[\frac{dE(T_0) - T_0\, dE(T_0)/dT}{kT}\right].$$

A negative $dE(T_0)/dT$ simultaneously increases the measured activation energy and the apparent collision factor. On the other hand, there are among glass forming materials rare exceptions, some of them organic, that do display Boltzmann behaviour of the viscosity above the glass transition temperature and, in addition, an unusually small jump in specific heat at this temperature [20].

The strong dependence of the switching time on voltage V is also puzzling. The data of figure 10 may be approximated by power laws $\tau \sim V^{-p}$ where p varies from 2 to 5 between the highest (111°C) and the lowest (60°C) temperatures, respectively. In contrast, the switching time of ferroelectric smectics is known to be inversely proportional to voltage ($p = 1$) [21]. Unlike tilted smectics, columnar liquid crystals cannot smoothly change their tilt direction because the elliptic columns obstruct each other during rotation or internal restructuring. Switching by field driven migration of pre-existing boundaries between differently oriented regions may be expected to result in $p = 1$. Also, this mechanism should give rise to large differences between samples and regions in a sample which were not noticed. We consider it more likely that ferroelectric switching starts from many thermally activated nucleation centres.

5. Conclusions

The occurrence of two columnar phases, depending on electric field strength, has permitted us to draw from the experimental data rather specific conclusions about their lattices of elliptic and polar columns. The fact that the ferroelectric polarization is three times larger in the high field than in the low-field phase agrees precisely with certain types of lattices and is incompatible with all others. The selection was confirmed by a relationship between the switching angle and elements of the optical dielectric tensor for which we assumed a simple form. For the present purposes, it was enough to verify that this relationship yields the same tilt angle of the molecular aromatic cores for both phases. However, the analysis based on the switching angles seems no less conclusive than the more direct approach starting from the ratio of polarizations. Additional clues have been used to narrow down further the number of possible lattices. At present we are trying to check our tentative assignments by X-ray diffraction.

Switchable ferroelectric columnar liquid crystals seem in some respects superior to ferroelectric smectics as regards electro-optical displays. They are probably more shock resistant, since they are stabilized by the two-dimensional lattice of columns that prevents circular flow. In addition, the alignment of the columns parallel to the electrodes rules out a chevron structure and the lattice of parallel columns inhibits a helical arrangement of tilt directions [15]. A fourth advantage of ferroelectric columnar mesophases over their smectic analogues could be tilt angles that hardly change with temperature (see figure 8). Finally, the optical tilt angle can be arrested for long periods at any intermediate value, so that multistable switching seems possible.

There are also some obvious disadvantages of columnar order as compared to smectic layers. Shearing is necessary to achieve a uniform alignment of the columns, and the

existence of columns is accompanied by new types of defects. The quality of alignment achievable and the role of defects in aligning and switching remain to be studied. The long switching times and their strong dependence on temperature are drawbacks which may be related to the particular material. We hope especially that ferroelectric columnar liquid crystals switchable at room temperature will soon be available.

We wish to thank G. Heppke for his generous support, D. Bennemann, J. Bömelburg, J.-M. Hollidt, D. Lötzsch, H. Molsen, H. Schmidt and K. Wuthe for continuous help, G. Scherowsky and X. Chen for stimulating discussions, and the Deutsche Forschungsgemeinschaft for financing this work in part through Sfb 335.

References

[1] SCHADT, M., and HELFRICH, W., 1971, *Appl. Phys. Lett.*, **18,** 127.
[2] MEYER, R. B., LIEBERT, L., STRZELECKI, L., and KELLER, P., 1975, *J. Phys. Lett.*, **36,** L-69.
[3] CLARK, N. A., and LAGERWALL, S. T., 1980, *Appl. Phys. Lett.*, **36,** 899.
[4] CHANDRASEKHAR, S., SADASHIVA, B. K., and SURESH, K. A., 1977, *Pramana*, **9,** 471.
[5] PROST, J., 1981, *Comptes rendus du Colloque Pierre Curie: Symmetries and Broken Symmetries*, edited by N. Boccara (IDSET).
[6] LEVELUT, A. M., OSWALD, P., GHANEM, A., and MALTHÊTE, J., 1984, *J. Phys., Paris*, **45,** 745.
[7] PALFFY-MUHORAY, P., LEE, M. A., and PETSCHEK, R. G., 1988, *Phys. Rev. Lett.*, **60,** 2303.
[8] BOCK, H., and HELFRICH, W., 1992, *Liq. Crystals*, **12,** 697.
[9] RITCHIE, E., 1944, *J. Proc. R. Soc. N.S.W.*, **78,** 134.
[10] MUSGRAVE, O. C., and WEBSTER, C. J., 1971, *J. chem. Soc.*, 1393.
[11] FRANK, F. C., and CHANDRASEKHAR, S., 1980, *J. Phys., Paris*, **41,** 1285.
[12] ITOH, I., TANAKA, A., FUKUDA, F., and MIYAMOTO, T., 1991, *Liq. Crystals*, **9,** 221.
[13] SKARP, K., DAHL, I., LAGERWALL, S. T., and STEBLER, B., 1984, *Molec. Crystals liq. Crystals*, **114,** 283.
[14] MIYASATO, K., ABE, S., TAKEZOE, H., FUKUDA, A., and KUZE, E., 1983, *Jap. J. appl. Phys.*, **22,** L661.
[15] SKARP, K., and HANDSCHY, M. A., 1988, *Molec. Crystals liq. Crystals*, **165,** 439.
[16] DE GENNES, P. G., 1983, *J. Phys. Lett., Paris*, **44,** L657.
[17] LEVELUT, A. M., 1983, *J. Chim. phys.*, **80,** 149.
[18] BILLARD, J., DUBOIS, J. C., VAUCHER, C., and LEVELUT, A. M., 1981, *Molec. Crystals liq. Crystals*, **66,** 115.
[19] LEISEN, J., WERTH, M., BOEFFEL, C., and SPIESS, H. W., 1992, *J. chem. Phys.*, **97,** 3749.
[20] ANGELL, C. A., 1991, *J. non-crystalline Solids*, **13,** 131.
[21] SKARP, K., and ANDERSSON, G., 1986, *Ferroelectrics Lett. Sect.*, **6,** 67.